NASA Technical Paper 1339

Anisotropic Friction and Wear of Single-Crystal Manganese-Zinc Ferrite in Contact With Itself

Kazuhisa Miyoshi and Donald H. Buckley

OCTOBER 1978

NASA

NASA Technical Paper 1339

Anisotropic Friction and Wear of Single-Crystal Manganese-Zinc Ferrite in Contact With Itself

Kazuhisa Miyoshi
Kanazawa University
Kanazawa, Japan
and
Donald H. Buckley
Lewis Research Center
Cleveland, Ohio

National Aeronautics
and Space Administration

**Scientific and Technical
Information Office**

1978

SUMMARY

Sliding friction experiments were conducted to determine the anisotropic friction and wear of single-crystal manganese-zinc ferrite {100}, {110}, {111}, and {211} planes sliding against themselves. All experiments were conducted with loads of about 0.2 newton (20 g), at a sliding velocity of 3 millimeters per minute for a total sliding distance of 2.5 millimeters, in a vacuum of 10^{-8} N/m^2, and at a temperature of 25° C.

Mating the highest-atomic-density directions, ⟨110⟩, of matched crystallographic planes resulted in the lowest coefficients of friction. Thus, direction is important in the friction behavior of ferrites. Mating matched parallel high-atomic-density planes and crystallographic directions resulted in low coefficients of friction. Mating dissimilar crystallographic planes, however, did not give significantly different friction results from those with matched (same) planes.

Sliding caused cracking and the formation of hexagonal- and rectangular-platelet wear debris on the manganese-zinc ferrite surfaces, primarily from cleavage of {110} planes on the surface and in the bulk of the manganese-zinc ferrite.

INTRODUCTION

Manganese-zinc ferrite is becoming increasingly important as a magnetic material in highly developed magnetic recording devices (e.g., video tape recorders). The use of single-crystal and hot-pressed manganese-zinc ferrite in magnetic heads for industrial and home video and audio tape recorders has played a role in the explosion of magnetic recording technology. The ferrite is used, practically, in both single-crystal and polycrystalline (hot pressed) form.

Understanding the properties of crystalline ceramics requires an understanding of the properties of single crystals. The nature of the atomic arrangements and the location of atoms in a crystal lattice are basic to the properties of single crystals. The crystal structure of manganese-zinc ferrite is that of the spinels, as is illustrated in figure 1 (refs. 1 and 2). Oxygen ions are in a nearly close-packed cubic array. However, the distribution of the cations, such as Fe^{3+}, Mn^{2+}, and Zn^{2+}, in the available sites must be determined experimentally. This distribution influences not only the magnetic properties of manganese-zinc ferrite but also its mechanical properties and slip systems. For example, Hornstra (ref. 3) has investigated theoretically the dislocation structures in spinels on the assumption that {111} planes are the highest-atomic-density

planes and the preferred slip planes. According to his theory, dislocations with {111} slip planes may consist of four partial dislocations separated by three stacking faults. However, Lewis's electron microscopic study on the spinel magnesium aluminate ($MgAl_2O_4$) and Mizushima's etch pit study on the spinel manganese ferrite ($MnFe_2O_4$) suggest that slip occurs on the {110} planes (refs. 4 and 5).

We have conducted experiments to determine the tribophysical properties of single-crystal and polycrystalline manganese-zinc ferrite with the spinel structure in contact with various metals (ref. 6). We are also particularly interested in the influence of the crystallographic orientation of manganese-zinc ferrite on its adhesive friction-and-wear behavior. Therefore, as described in this paper, we examined the anisotropic nature of the friction-and-wear behavior of single-crystal manganese-zinc ferrite {100}, {110}, {111}, and {211} surfaces sliding against themselves. All experiments were conducted with loads of about 0.2 newton (20 g), at a sliding velocity of 3 millimeters per minute for a total sliding distance of 2.5 millimeters, in a vacuum of 10^{-8} N/m^2, and at a temperature of 25° C.

MATERIALS

The as-grown platelets of single-crystal manganese-zinc ferrite used in these experiments were 99.9 percent pure oxide. The composition and hardness data on manganese-zinc ferrite are described in reference 6 and presented in table I. The crystal structure of manganese-zinc ferrite is illustrated in figure 1. In the unit cell, which contains 32 oxygen ions, there are 32 octahedral sites and 64 tetrahedral sites. Sixteen of the octahedral sites are filled with equal amounts of divalent (Mn^{2+}, Zn^{2+}, Fe^{2+}) and trivalent (Fe^{3+}) ions, and eight of the tetrahedral sites are filled with trivalent (Fe^{3+}) ions (refs. 1 and 2).

APPARATUS

The experiments were conducted in a vacuum chamber. The vacuum chamber contained a system that measured adhesion, load, and friction and performed Auger and low-energy electron diffraction (LEED) surface analysis. The mechanism for applying load and measuring adhesion and friction is shown in figure 2. A gimbal-mounted beam projected into the vacuum system. The beam contained two flats machined normal to each other on which strain gages were mounted. The end of the beam contained the single-crystal manganese-zinc ferrite rider specimen. The load was applied by moving the beam toward the flat disk and was measured by one of the strain gages. The rider was moved tangentially along the flat disk by means of the gimbal assembly. Under an

applied load, the friction force was sensed by the strain gage normal to that used to measure the applied load. Rider sliding was as indicated in figure 2. The vacuum apparatus in which the components of figure 2 were contained also had a LEED diffraction system and an Auger spectrometer. The electron beam of both could be focused on any disk site by means of a disk-manipulation device. The vacuum system was a conventional vacsorb and ion-pumped system capable of readily achieving pressures of 1.33×10^{-8} N/m^2 (10^{-10} torr) as measured by a nude ion gage within the specimen chamber. Sublimation pumping was also used to more rapidly achieve the desired pressure.

EXPERIMENTAL PROCEDURE

Specimen Preparation

The surfaces of the single-crystal manganese-zinc ferrite rider specimens were hemispherical and were polished with approximately 3-micrometer-diameter diamond powder and then 1-micrometer-diameter aluminum oxide (Al_2O_3) powder. The orientations of the single-crystal manganese-zinc riders are shown in figure 3(a) to an accuracy of $\pm2^{\circ}$. For the {100} orientation at the interface, the {100} plane of the rider specimen was oriented such that it was nearly parallel to the sliding interface. For the {110} and {111} orientations, rider specimens were also oriented as indicated in figure 3(a). The radius of curvature of the riders was 0.79 millimeter (1/32 in.).

The surfaces of the single-crystal manganese-zinc ferrite disk specimens were also polished with 3-micrometer-diameter diamond powder and then 1-micrometer-diameter aluminum oxide powder. The orientations of the single-crystal manganese-zinc ferrite disks are shown in figure 3(b) to an accuracy of $\pm1^{\circ}$. For the {100} orientation at the interface, the {100} plane of the disk specimen was oriented such that it was nearly parallel to the sliding interface. For the {110}, {111}, and {211} orientations, disk specimens were also oriented as indicated in figure 3(b). The method used for determining the orientation of single crystals was the back-reflection Laue method.

Both disks and riders of manganese-zinc ferrite were also chemically polished with hydrochloric acid at $50^{\circ}\pm1^{\circ}$ C for 2 minutes after the mechanical polishing. However, the friction properties of the chemically and mechanically polished surfaces were not significantly different. These experiments were conducted to establish the deformation effects of mechanical polishing on friction.

Procedure

The surfaces of the disk and rider specimens were rinsed with absolute ethyl alcohol before the experiment. For the experiments in vacuum, the specimens were placed in the vacuum chamber and the system was evacuated and baked out to achieve a pressure of 10^{-8} N/m^2 (10^{-10} torr). When this vacuum was achieved, argon gas was bled back into the vacuum chamber to a pressure of 1 N/m^2. A 1000-volt, direct-current potential was applied and the specimens (disk and rider) were argon sputter bombarded for 30 minutes. The vacuum chamber was then reevacuated, and Auger spectra of the disk surface were obtained to determine the degree of surface cleanliness. When the disk surface was clean, friction experiments were conducted.

A load of about 0.2 N (20 g) was applied to the rider-disk contact by deflecting the beam shown in figure 1. Both load and friction force were continuously monitored during a friction experiment. Sliding velocity was 3 millimeters per minute for a total sliding distance of 2.5 millimeters. All friction experiments in vacuum were conducted with the system reevacuated to a pressure of 10^{-8} N/m^2.

RESULTS AND DISCUSSION

Auger Analysis of Manganese-Zinc Ferrite Surfaces

Auger spectra of the as-received, single-crystal manganese-zinc ferrite surface were obtained before and after sputter cleaning. The spectra obtained before sputter cleaning revealed a carbon contamination peak in addition to the oxygen and iron. An Auger spectrum for a manganese-zinc ferrite {110} surface after sputter cleaning is shown in figure 4. The carbon contamination peak has completely disappeared from the spectrum. In addition to oxygen and iron, Auger peaks indicate small amounts of manganese and zinc on the surface. Comparing the oxygen-to-iron peak height ratios of the {100}, {110}, {111}, and {211} surfaces reveals that the surface accommodated slightly more oxygen with the {110} plane than with the {211}, {111}, and {100} planes, in that order.

Friction Behavior

Matched crystallographic planes in contact. - Sliding friction experiments were conducted with the {100}, {110}, and {111} planes of manganese-zinc ferrite riders inclined at various angles with respect to the mated manganese-zinc ferrite disk. The results are shown in figure 5. For these tests, all disks were turned relative to the rider

on an axis in the ⟨110⟩ direction of the rider to achieve the desired orientation, and sliding was in the ⟨110⟩ direction on both riders and disks. The data of figure 5 indicate that the coefficient of friction was lowest with the plane of the rider parallel to the interface, that is, at an angle of zero degrees to the sliding mating surface. The reason is that a higher atomic density interface is achieved with parallel planes than with surfaces inclined at various angles. This is consistent with earlier studies (refs. 7 and 8). The coefficients of friction reported herein were obtained from measurements of three to five friction traces. The deviation in friction with repeated experiments was ±10 percent of that indicated in the figure.

The coefficients of friction for these three crystallographic planes of manganese-zinc ferrite - {100}, {110}, and {111} - in contact with themselves did not differ significantly. It might be anticipated from these results that the atomic densities for the {100}, {110}, and {111} planes are all very high because the distribution of the cations in the available sites is very complicated in a spinel crystal, as shown in figure 1.

Dissimilar crystallographic planes in contact. - Sliding friction experiments were conducted with the {110} planes of manganese-zinc ferrite riders inclined at various angles with respect to the {100}, {111}, or {211} plane of the mated manganese-zinc ferrite disk. The results are shown in figure 6. For these tests, all disks were turned on an axis in the ⟨110⟩ direction of the rider, and all sliding was in the ⟨110⟩ direction on both riders and disks. The data of figure 6 reveal that the coefficients of friction for the three sets of dissimilar crystallographic planes - {110} on {100}, {110} on {111}, and {110} on {211} - were nearly the same as those for the three sets of matched crystallographic planes (fig. 5). However, in figure 6, as anticipated, there is no friction minimum when the rider is parallel to the disk surface.

Dissimilar crystallographic directions in contact. - Experiments were also conducted with the {110} rider sliding on flat surfaces of the {110}, {111}, and {211} planes, but in dissimilar crystallographic directions to that of the rider. Sliding was in the ⟨110⟩ direction on the rider, in the ⟨100⟩ direction on the {110} surface of the disk, in the ⟨211⟩ direction on the {111} surface of the disk, and in the ⟨111⟩ direction on the {211} surface of the disk. The ⟨110⟩ directions are generally the highest-atomic-density directions on the low Miller index plane in a spinel crystal. The data are presented in figure 7. The coefficients of friction for the three sets of mated crystallographic planes sliding in these dissimilar directions were generally higher than those shown in figures 5 and 6 and varied according to the angle at which the surface of the rider was inclined. The coefficient of friction was lowest with the {110} of rider parallel to the interface, that is, at an angle of zero degrees to the sliding disk surface.

Examination of figures 5 to 7 suggests that the lowest coefficients of friction were obtained with the high-atomic-density planes (low Miller index planes) and with the highest-atomic-density crystallographic direction. The subject is discussed in detail in the next section.

Comparison of sliding in the same and dissimilar directions. - It might be anticipated from the preceding results that mating the same crystallographic direction on both rider and disk would cause a significant difference in the coefficient of friction. The coefficients of friction for three sets of mated crystallographic planes sliding in the same and dissimilar directions are replotted in figure 8. Sliding friction experiments were also conducted with the {100} plane of the rider in sliding contact with the {110} plane of the disk (fig. 9). The differences in coefficients of friction with respect to the crystallographic directions are significant in the results of figures 8 and 9. Mating both ⟨110⟩ directions resulted in lower coefficients of friction than mating the other directions. The ⟨110⟩ directions are generally the highest-atomic-density directions, as already mentioned. The ⟨110⟩ direction on the {110} plane is the preferred slip direction (ref. 5). Thus, mating the highest-atomic-density directions on matched crystallographic planes (fig. 8(a)) resulted in the lowest coefficient of friction. These results indicate that mating the same crystallographic directions can play a significant role in the friction behavior of manganese-zinc ferrite. Mating the high-atomic-density planes may also result in a low coefficient of friction.

Wear Behavior

After the single-pass experiments described in the preceding section were completed, multipass experiments were conducted to establish steady-state conditions. When repeated passes were made of the manganese-zinc ferrite rider over the same manganese-zinc ferrite surface at a load of 0.2 newton (20 g), the coefficient of friction either remained constant or increased slightly with repeated passes. The friction traces for repeated passes were all characterized by stick-slip behavior.

The wear behavior of manganese-zinc ferrite surfaces was observed with respect to cracking and the wear debris generated by fracture.

Cracking. - The sliding contact of manganese-zinc ferrite surfaces results in surface cracks along the {110} planes. Figure 10 shows scanning electron micrographs of the rider wear scar and the disk wear track as a result of five passes of the rider on the same disk surface. The {110} plane of the rider and the {211} plane of the disk were parallel to the sliding interface. Small cracks that zig-zag along cleavage planes of the {110} plane are clearly evident on both rider and disk. Such small cracks propagated along cleavage planes of the {110} plane and were observed on the surfaces of other riders and disks, such as the {100} and {111} planes.

Figure 11 shows a scanning electron micrograph of the cracks propagated along the {110} planes and a fracture pit on the rider as a result of 20 passes over the manganese-zinc ferrite {110} surface. A fracture pit is formed primarily because of cleavage cracking and subsurface cracking along the {110} planes. The smooth surface

at the bottom of a fracture pit is due to subsurface cleavage of the {110} planes. Thus, the fracture behavior of manganese-zinc ferrite crystals during sliding depends significantly on the cleavage systems of the {110} planes.

Wear debris. - It might be anticipated from figures 10 and 11 that the wear debris would be polygon-shaped platelets, the sides of which are produced by cleavage cracking. Two types of wear debris were observed: hexagonal and rectangular platelets. Figure 12 shows the wear particles of the rider transferred to the surface of a disk. The {110} planes of both the rider and the disk were parallel to the sliding interface. The wear particles are nearly full, as well as partial, hexagonal platelets and are flat. Hexagonal platelets form because of cleavage of the {110} planes, where the angles between different {110} planes on a {110} sliding surface are 60° or common multiples thereof. Flat platelets form because of cleavage of {110} planes in the bulk, parallel to the sliding interface.

The second type of wear debris is rectangular platelets. Figure 13 shows a dislodged wear particle of the disk, with its fracture surface exposed. The {100} plane of the disk was parallel to the sliding interface. The wear particle has a nearly rectangular shape. The exposed fracture surfaces of the wear debris have cleavage steps. The risers of the steps may be {110} planes. Because the ledges of steps are very smooth, the ledges may have been formed by subsurface cracking of the {110} planes in the disk. Rectangular platelets form because of cleavage of the {110} planes, where the angles between different {110} planes on the {100} sliding surface are 90° or common multiples thereof. Thus, hexagonal- and rectangular-platelet wear debris may be produced by cleavage systems of the {110} planes.

CONCLUSIONS

From the sliding friction experiments conducted in this investigation with single-crystal manganese-zinc ferrite {100}, {110}, {111}, and {211} surfaces in sliding contact with themselves, the following conclusions were drawn:

1. Mating the highest-atomic-density directions, ⟨110⟩, on matched crystallographic planes resulted in the lowest coefficient of friction, indicating that direction is important in the friction behavior of ferrites.

2. Mating surfaces with matched parallel high-atomic-density planes and matched crystallographic directions at the interface resulted in low coefficients of friction. Mating dissimilar crystallographic planes, however, did not give a significant difference in friction from that observed with matched planes.

3. Sliding caused cracking and the formation of hexagonal- and rectangular-platelet wear debris on the manganese-zinc ferrite surfaces, primarily because of cleavage of the {110} planes on the surface and in the bulk of the manganese-zinc ferrite.

Lewis Research Center,
National Aeronautics and Space Administration
Cleveland, Ohio, June 28, 1978,
506-16.

REFERENCES

1. Von Hippel, Arthur R.: Dielectrics and Waves. John Wiley & Sons, Inc., 1954, pp. 219-228.

2. Kingery, W. D.; Bowen, H. K.; and Uhlmann, D. R.: Introduction to Ceramics. Second ed. John Wiley & Sons, Inc., 1976, pp. 25-88 and pp. 975-1015.

3. Hornstra, J.: Dislocations, Stacking Faults and Twins in the Spinel Structure. J. Phys. Chem. Solids, vol. 15, 1960, pp. 311-323.

4. Lewis, M. H.: Defects in Spinel Crystals Grown by the Verneuil Process. Phil. Mag., vol. 14, no. 131, Nov. 1966, pp. 1003-1018.

5. Mizushima, Masahiro: Etch Pits in Manganese Ferrite Single Crystals. Jap. J. Appl. Phys., vol. 7, no. 8, Aug. 1968, pp. 893-898.

6. Miyoshi, Kazuhisa; and Buckley, Donald H.: Friction and Wear of Single-Crystal and Polycrystalline Manganese-Zinc Ferrite in Contact with Various Metals. NASA TP-1059, 1977.

7. Buckley, Donald H.: The Influence of the Atomic Nature of Crystalline Materials on Friction. ASLE Trans., vol. 11, no. 2, 1968, pp. 89-100.

8. Johnson, R. L.; and Buckley, Donald H.: Lubrication and Wear Fundamentals for High-Vacuum Applications. Proc. Inst. Mech. Eng. (London), vol. 182, pt. 3A, 1967-68, pp. 479-490.

TABLE I. - COMPOSITION AND HARDNESS DATA ON SINGLE-CRYSTAL MANGANESE-ZINC FERRITE

[Composition of manganese-zinc ferrite, wt %: Fe_2O_3, 71.6; MnO, 17.3; and ZnO, 11.1.]

Hardness	Surface							
	{100}		{110}		{111}		{211}	
	Direction							
	⟨001⟩	⟨011⟩	⟨001⟩	⟨110⟩	⟨112⟩	⟨110⟩	⟨111⟩	⟨011⟩
Knoop hardness[a]	630	560	630	560	580	600	550	580
Vickers hardness[b]	630	630	645	645	590	590	650	650

[a]Measuring load, 300 g.
[b]Measuring load, 50 g.

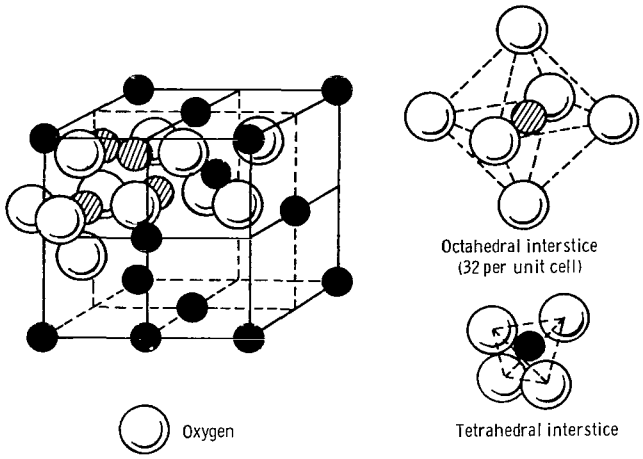

(a) Spinel structure.

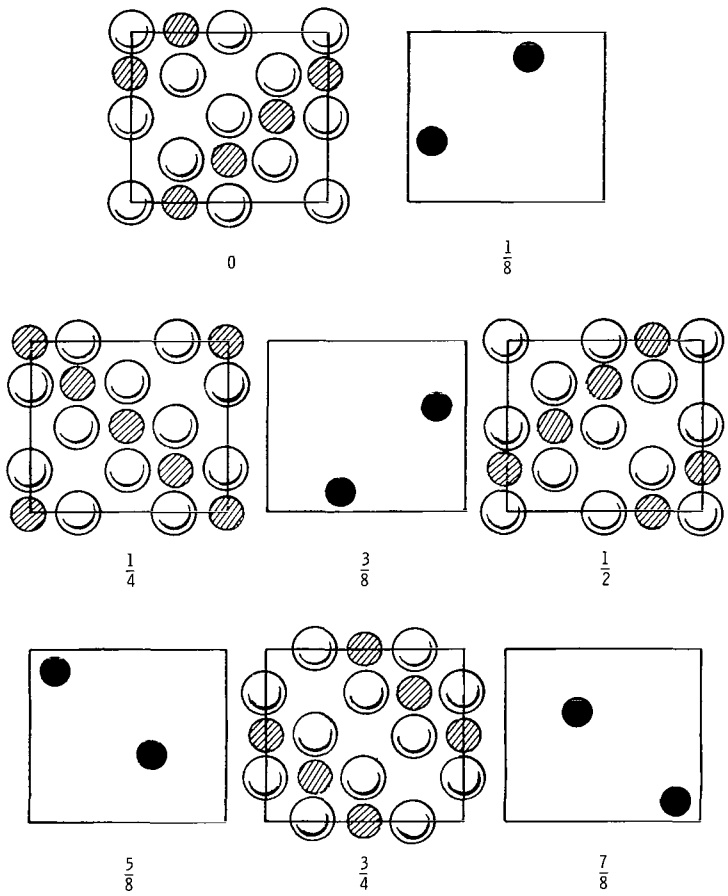

(b) Layers of atoms parallel to (100) plane.

Figure 1. - Spinel structure. (From refs. 1 and 2.)

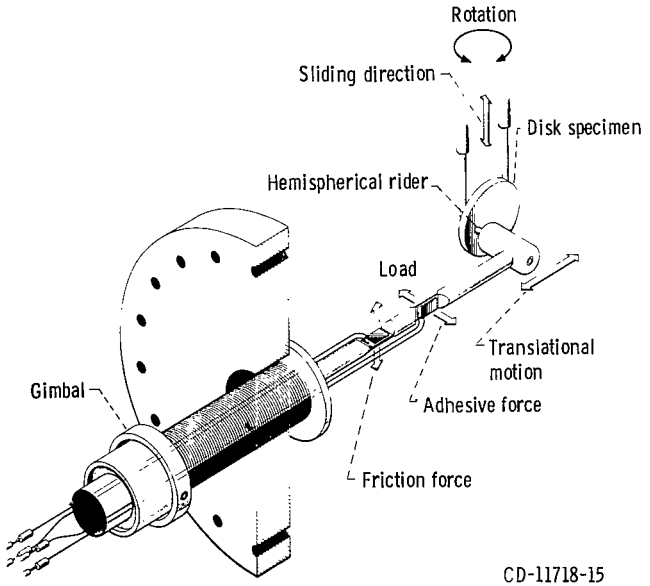

Figure 2. - High-vacuum friction-and-wear apparatus.

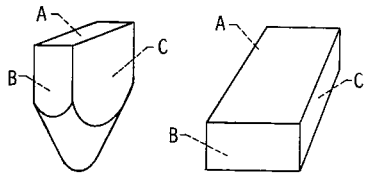

(a) Rider. (b) Disk.

Plane designation	Crystallographic plane			
A	{100}	{110}	{111}	{211}
B	{110}	{100}	{211}	{111}
C	{110}	{110}	{110}	{110}

Figure 3. - Orientation of single-crystal manganese-zinc ferrite riders and disks for sliding friction and wear tests in vacuum. ("A" plane parallel to sliding interface.)

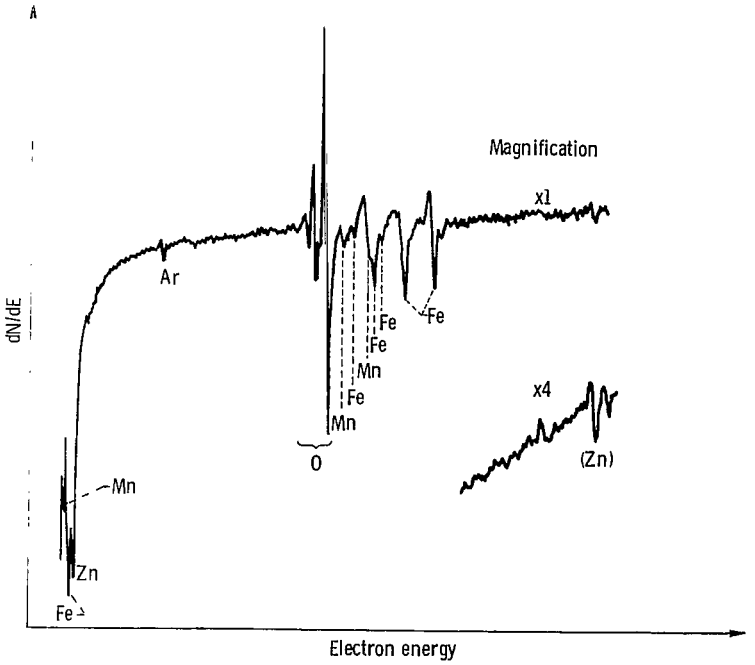

Figure 4. - Auger emission spectroscopy spectrum for manganese-zinc ferrite {110} surface after sputter cleaning.

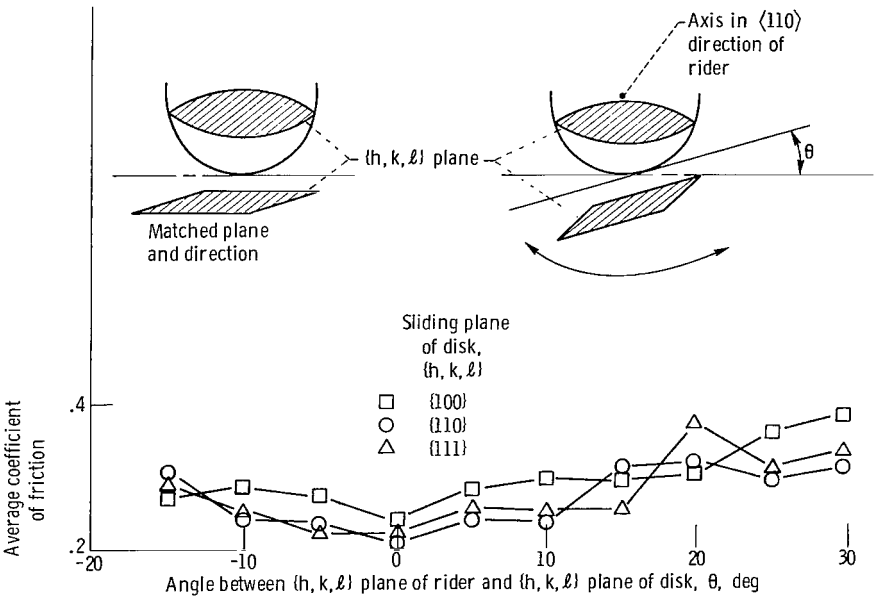

Figure 5. - Coefficient of friction as function of angle between {h, k, ℓ} plane of rider and {h, k, ℓ} plane of disk. Sliding direction for both riders and disks, ⟨110⟩; single pass; rider and disk material, manganese-zinc ferrite.

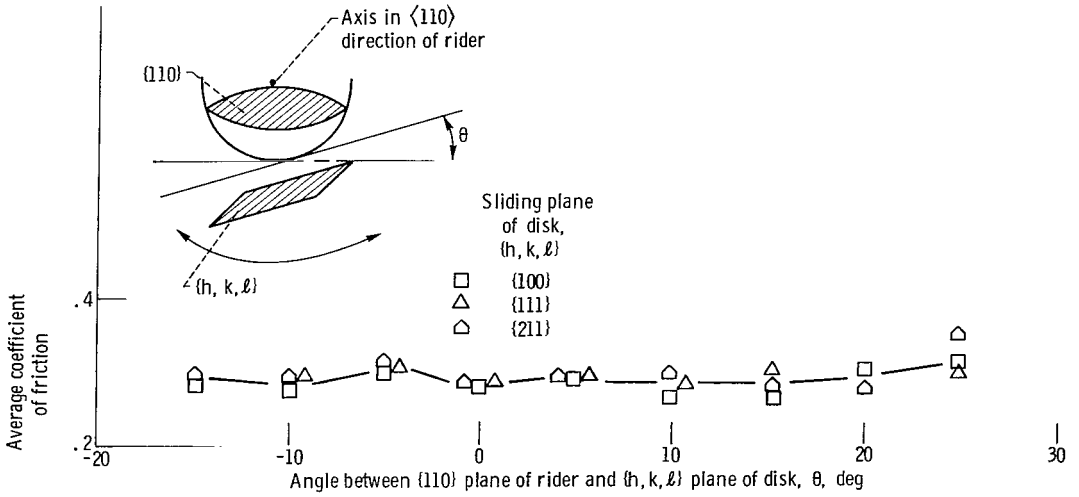

Figure 6. - Coefficient of friction as function of angle between {110} plane of rider and {h, k, ℓ} plane of disk. Sliding direction for both riders and disks, ⟨110⟩; single pass; rider and disk material, manganese-zinc ferrite.

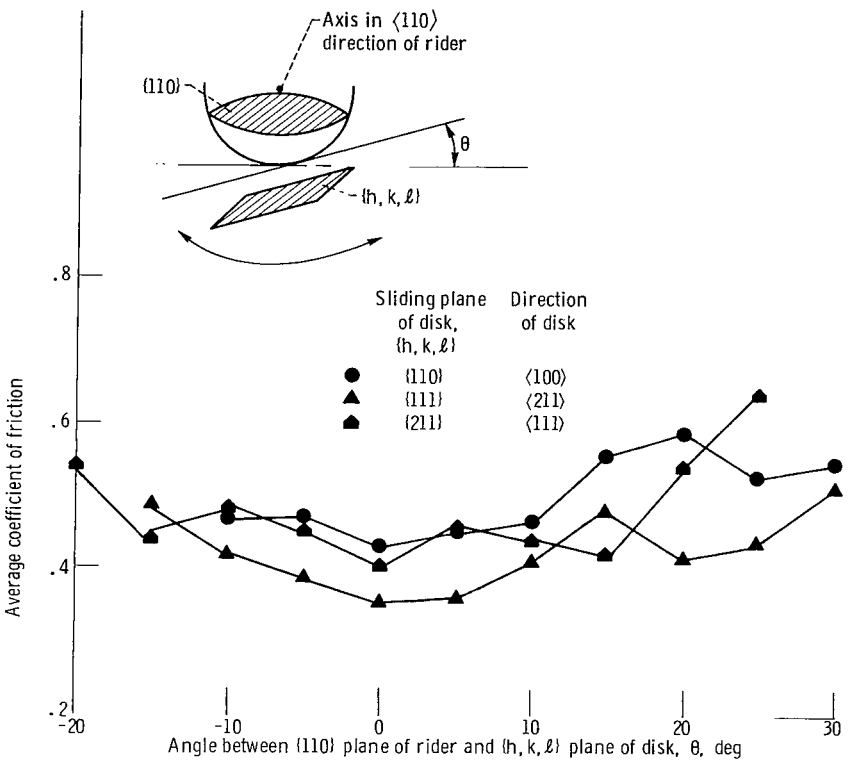

Figure 7. - Coefficient of friction as function of angle between {110} plane of rider and {h, k, ℓ} plane of disk. Sliding direction of rider, ⟨110⟩; single pass; rider and disk material, manganese-zinc ferrite.

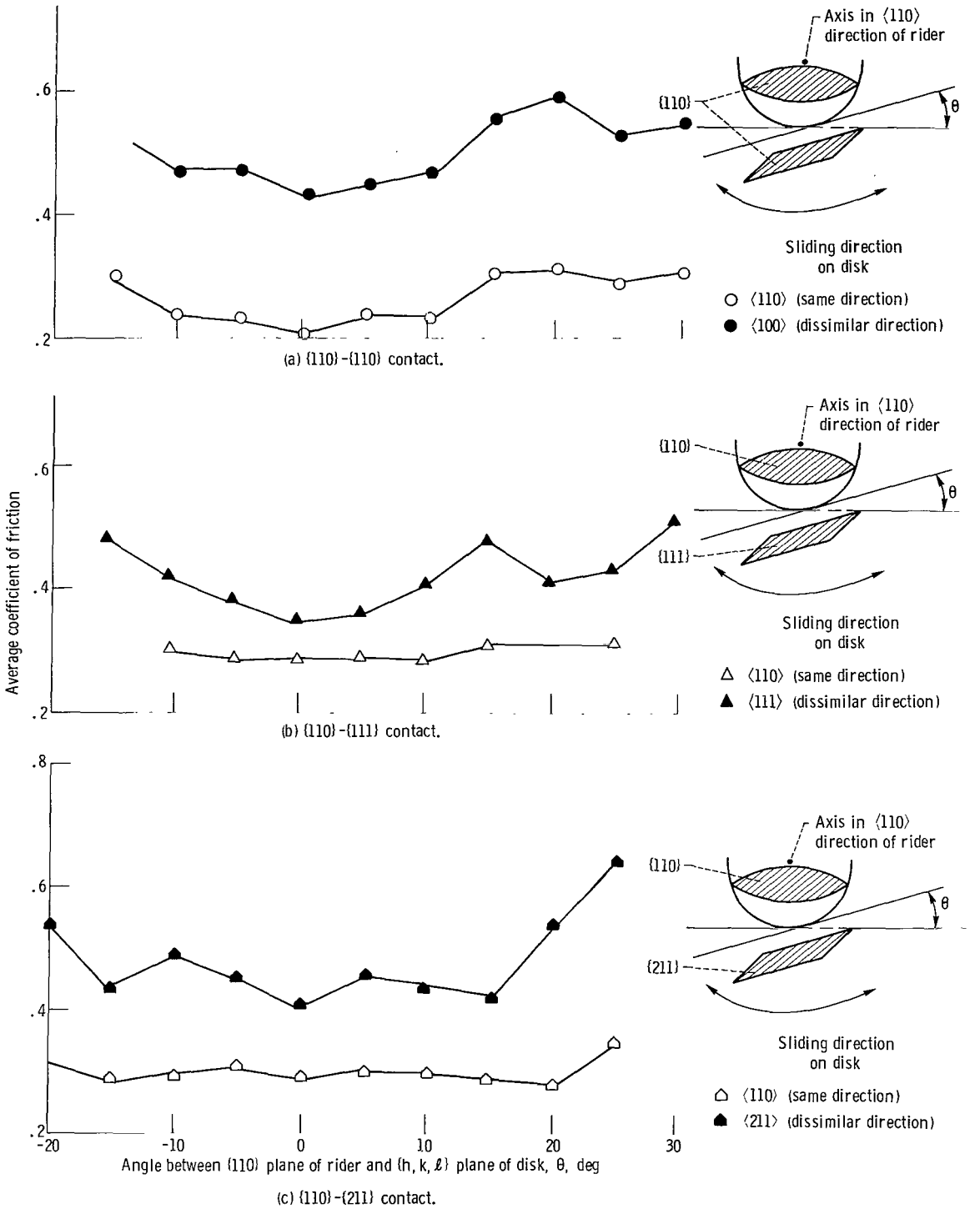

Figure 8. - Coefficients of friction for mating same and dissimilar directions of rider and disk. Sliding direction of rider, ⟨110⟩; single pass; rider and disk material, manganese-zinc ferrite.

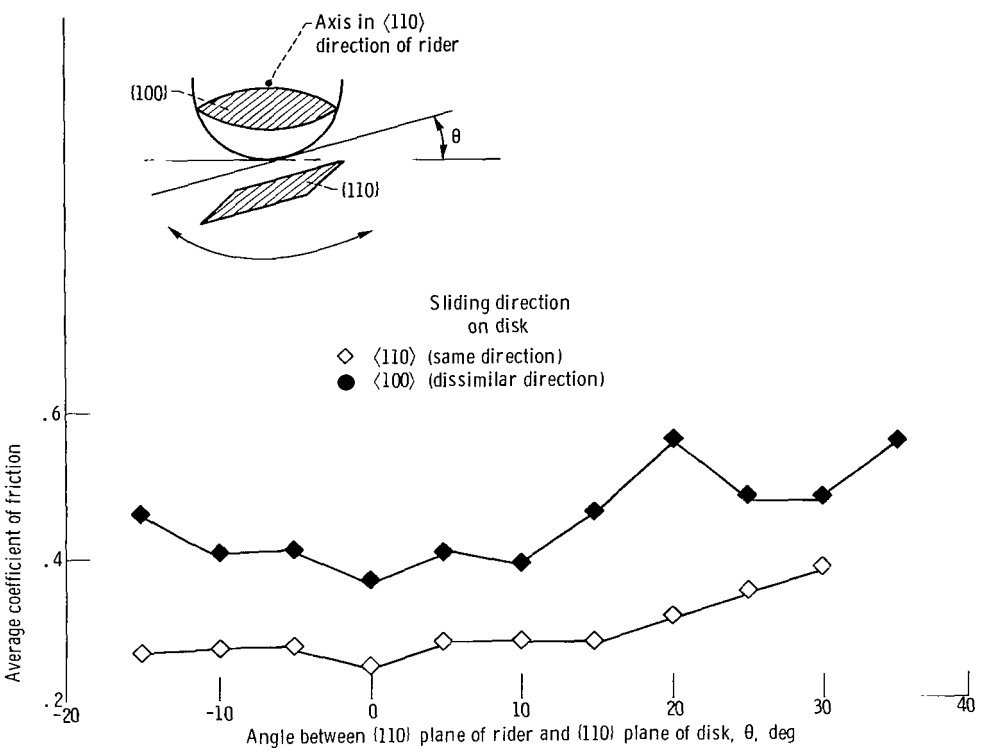

Figure 9. - Coefficients of friction for mating same and dissimilar directions of rider and disk. Sliding direction of rider, ⟨110⟩; single pass; rider and disk material, manganese-zinc ferrite.

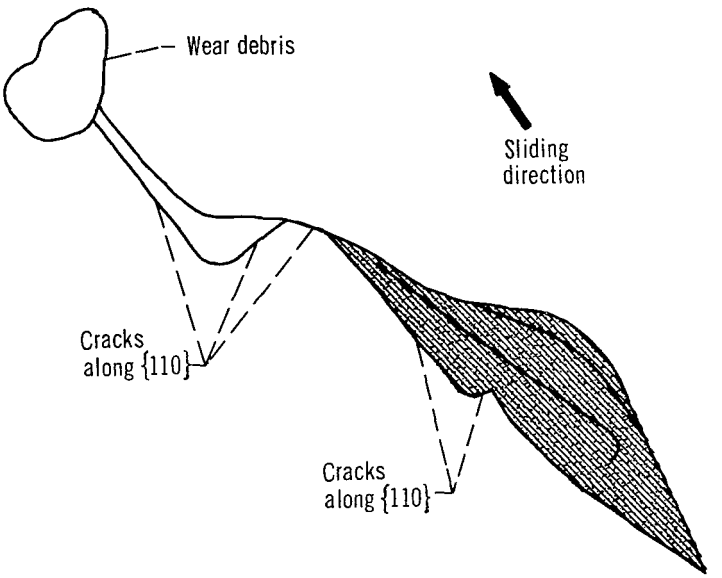

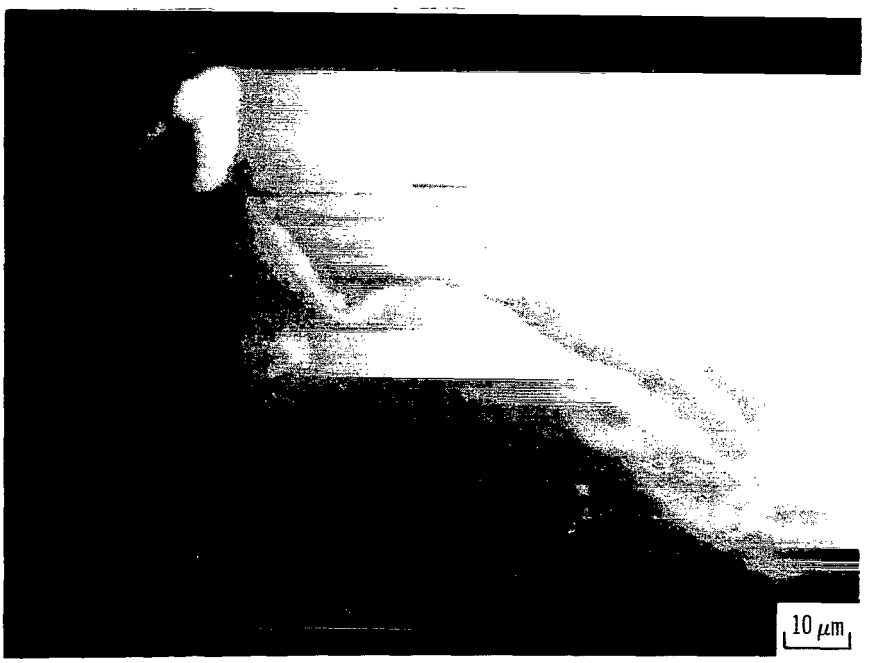

(a) Rider, with {110} plane parallel to interface.

Figure 10. - Scanning electron micrographs of cracking of single-crystal manganese-zinc ferrite {110} rider after 5 passes in sliding contact with single-crystal manganese-zinc ferrite {211} disk. Sliding direction for rider and disk, ⟨110⟩.

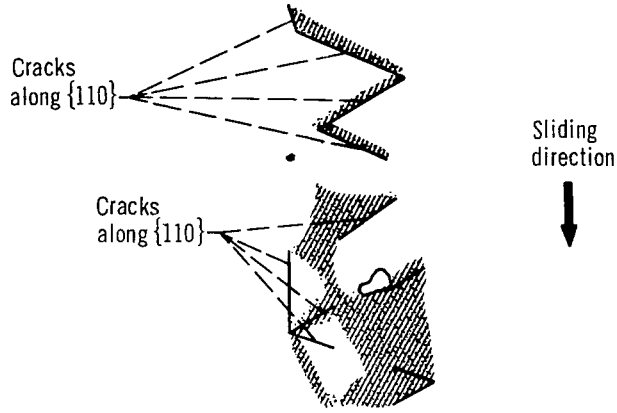

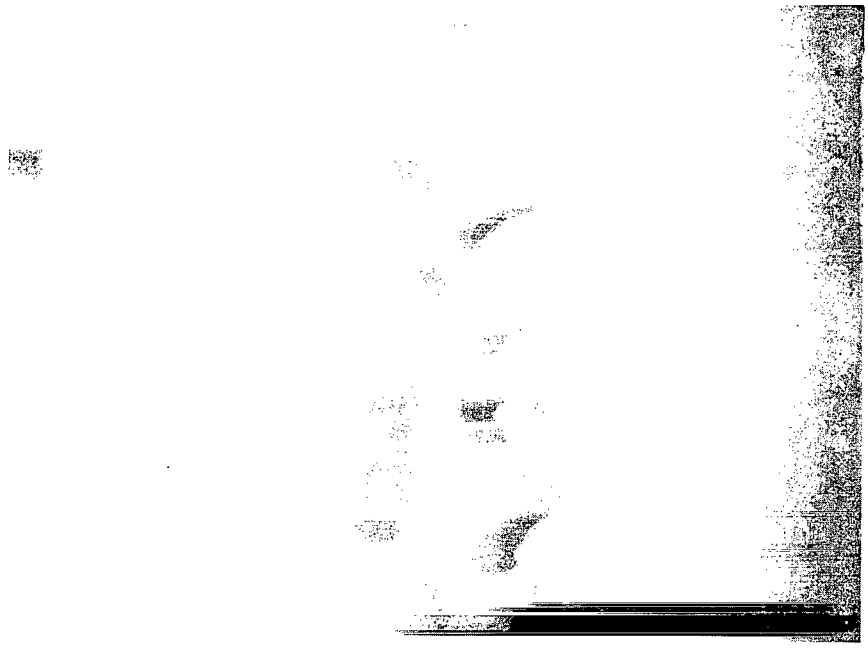

(b) Disk, with {211} plane parallel to interface.

Figure 10. - Concluded.

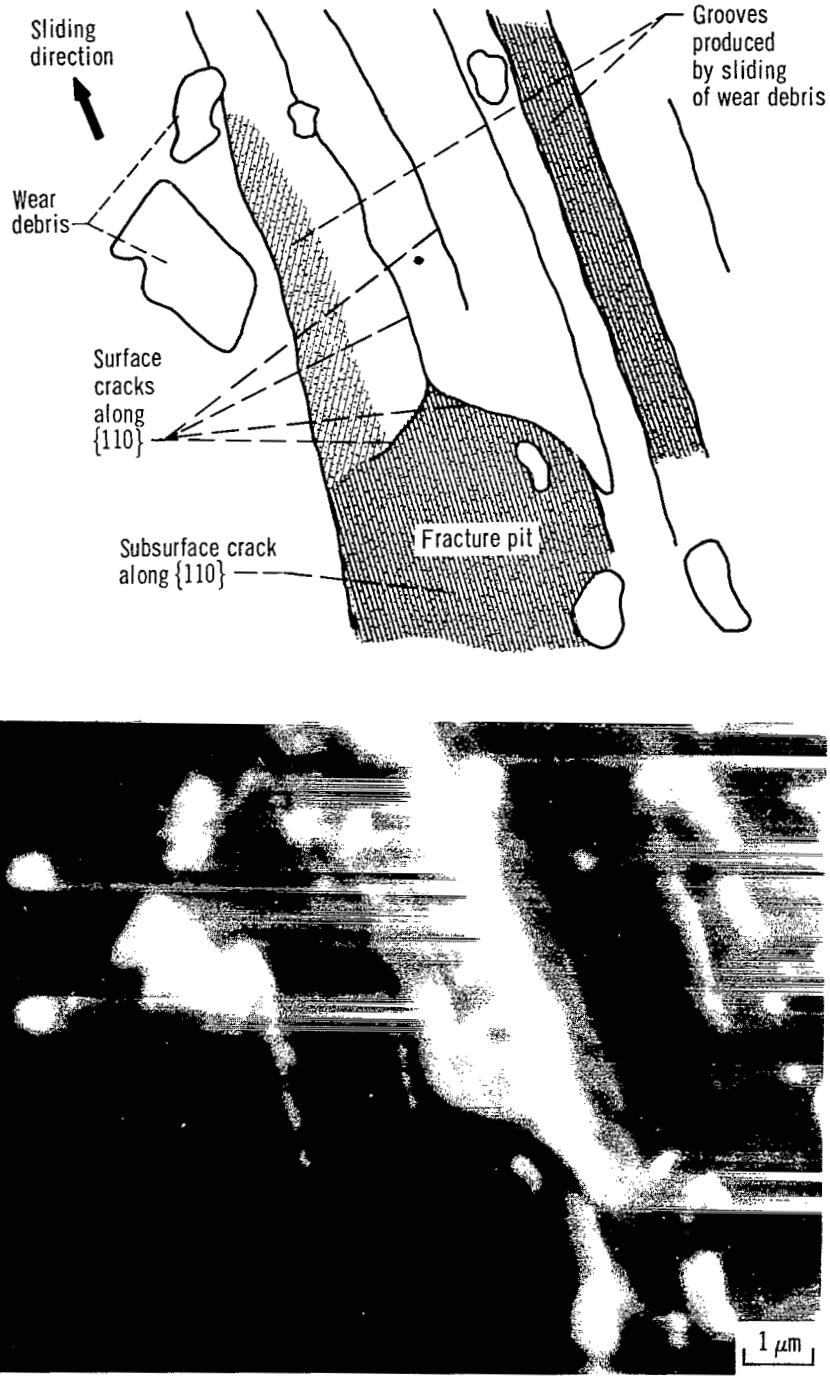

Figure 11. - Scanning electron micrograph of fracture pit and cracks on single-crystal manganese-zinc ferrite {110} rider after 20 passes in sliding contact with single-crystal manganese-zinc ferrite {110} disk. Sliding direction for rider and disk, ⟨110⟩.

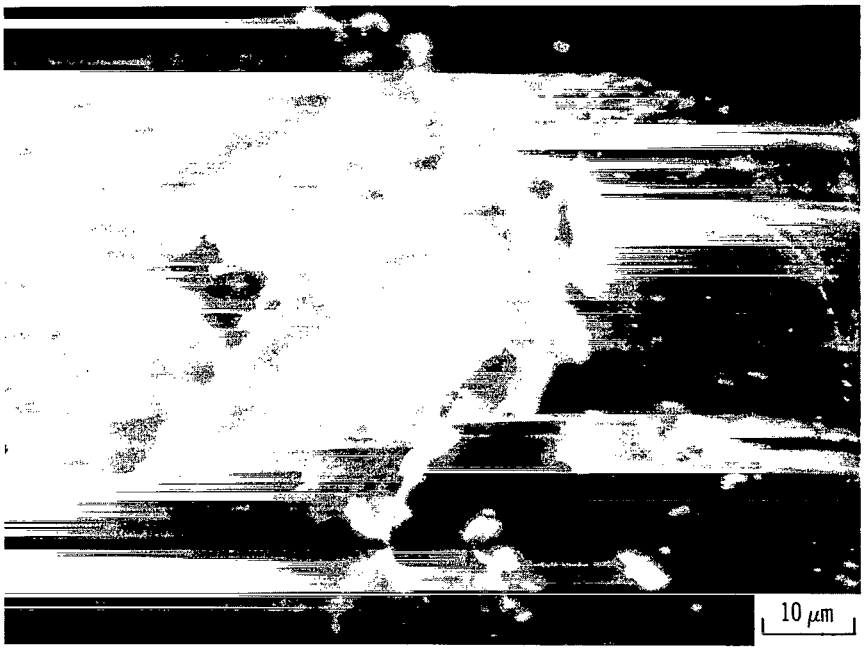

(a) Nearly completely hexagonal wear debris.

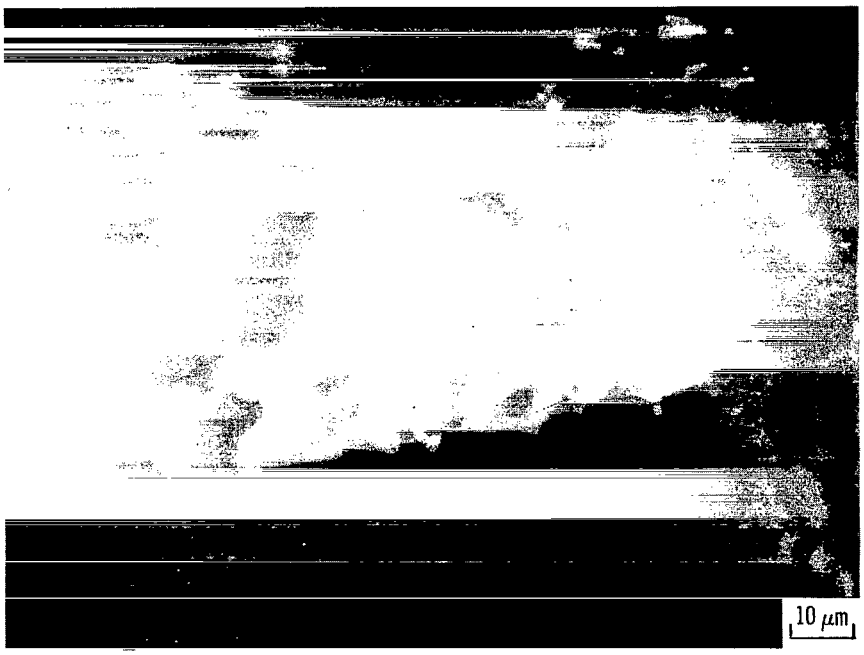

(b) Partially hexagonal wear debris.

Figure 12. - Scanning electron micrograph of wear track on single-crystal manganese-zinc ferrite {110} disk, showing transfer of hexagonal wear debris from single-crystal manganese-zinc ferrite {110} rider after 10 passes. Sliding direction for rider and disk, ⟨110⟩.

Figure 13. - Scanning electron micrograph of wear track on single-crystal manganese-zinc ferrite {100} disk, showing dislodged rectangular wear debris of disk after 10 passes in sliding contact with single-crystal manganese-zinc ferrite {110} rider. Sliding direction for rider and disk, ⟨110⟩.